

© 2025 IEEE

Proceedings of the 40th Applied Power Electronics Conference and Exposition (APEC 2025), Atlanta, GA, USA,
March 16-20, 2025

Comparative Analysis of Carbon Footprints and Material Usage of Solid-State Transformers and Low-Frequency-Transformer-Based MVac-LVdc Interfaces for High-Power EV Charging

L. Imperiali,
R. Wang,
A. Anurag,
P. Barbosa,
J. W. Kolar,
J. Huber

Personal use of this material is permitted. Permission from IEEE must be obtained for all other uses, in any current or future media, including reprinting/republishing this material for advertising or promotional purposes, creating new collective works, for resale or redistribution to servers or lists, or reuse of any copyrighted component of this work in other works

Comparative Analysis of Carbon Footprints and Material Usage of Solid-State Transformers and Low-Frequency-Transformer-Based MVac-LVdc Interfaces for High-Power EV Charging

Luc Imperiali*, Rudy Wang[†], Anup Anurag[†], Peter Barbosa[†], Johann W. Kolar*, and Jonas Huber*

*Advanced Mechatronics Systems Group, ETH Zurich, Switzerland

[†]Delta Electronics, Raleigh, USA

imperiali@ams.ee.ethz.ch

Abstract—Medium-voltage (MV) ac to low-voltage (LV) dc conversion for, e.g., high-power EV charging can be realized either with a low-frequency transformer (LFT) and a downstream LV ac-dc converter, or, alternatively, as a modular solid-state transformer (SST) that employs high-frequency (HF) transformers to provide galvanic isolation. Both solutions achieve similar power conversion efficiencies in the order of 98% but differ significantly regarding complexity and the types and amounts of employed components and materials. Thus, this paper compares the two approaches regarding the embodied carbon footprint and the material usage, on the basis of industrial 400 kW first-generation and 1200 kW second-generation SST demonstrators, highlighting the potential of SST technology to benefit from improvements in power electronics whereas the LFT-based solutions remain constrained by high material usage for the transformer. Specifically, the 1200 kW second-generation SST demonstrator features only about 40% of the mass (2 kg/kW) and about 2/3 of the embodied carbon footprint (13.7 kg CO₂eq/kW) of an equally rated LFT-based solution.

Index Terms—Carbon footprint, low-frequency transformer, LFT, material usage, medium voltage, MVac-LVdc, solid-state transformer, SST, transformer.

I. INTRODUCTION

High-power low-voltage (LV) dc loads, e.g., datacenters or EV fast chargers, are supplied from the medium-voltage (MV) ac mains. Conventionally, such MVac-LVdc interfaces are conventionally realized with a low-frequency (i.e., mains frequency of 50 Hz or 60 Hz) transformer (LFT) providing galvanic separation and voltage step-down, and a downstream LV ac-dc converter, see Fig. 1a. Aiming at a reduced weight and size, solid-state transformers (SSTs), where high-frequency (HF) transformers (HFTs) provide the galvanic separation, e.g., as shown in Fig. 1b, have been considered since the 1970s, in particular for weight-/space-constrained applications like traction [1]. However, given the opposing long-term trends of increasing raw material prices (in particular for copper) and declining prices for high-volume electronics production indicated in Fig. 2, more recently, SSTs have been also proposed for various stationary applications like datacenters [2], electrolysis [3], PV inverters [4], and high-power EV charging [5]–[8], for which industry has demonstrated full-scale prototype systems [9]–[11].

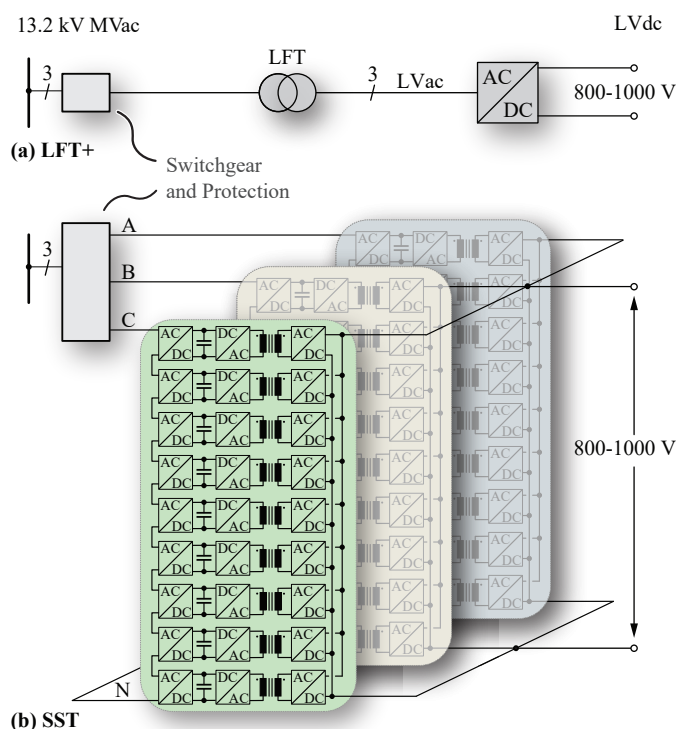


Fig. 1. MVac-LVdc interfaces realized (a) conventionally with a low-frequency transformer (LFT) and a LV-side ac-dc converter (denominated as “LFT+” in this paper) or (b) as a fully modular solid-state transformer (SST), where the galvanic isolation is provided by high-frequency transformers (HFTs) in the converter cells.

While economical considerations thus drive the interest in SST technology, the evermore visible signs of climate change and the certainty that resources are limited have lead to an increased environmental awareness in society. Thus, corresponding requirements for products are being codified in regulations like the European Union’s Green Deal [15] and Circular Economy Action Plan [16] or standards like IEC 62430 (Environmentally conscious design for electric and electronic products), etc. Such considerations are relevant for power electronics, too, and there are already manufacturers

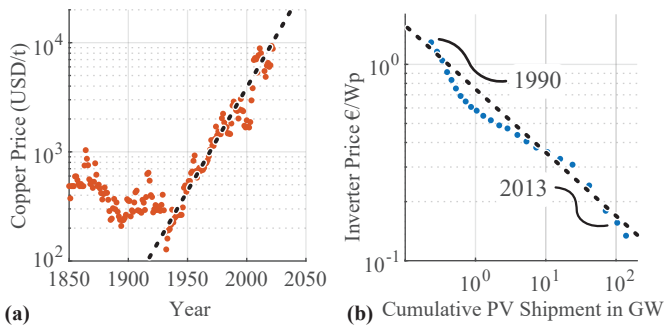


Fig. 2. (a) Increasing copper prices over the last 175 years [12], [13] and (b) learning curve of LV power electronics, specifically PV inverters [14]. Thus, costs of LFT-based solutions must be expected to increase whereas costs of modular SSTs potentially decrease in the future.

publishing life-cycle assessment (LCA) studies for their power converters [17]–[20], quantifying the environmental impacts resulting over the life cycle, i.e., from raw material sourcing through production, use phase, and finally waste disposal and/or recycling. Similarly, there is a growing body of scientific literature concerning LCAs, material efficiency, circular economy compatibility, etc. of power electronic converters [17], [21]–[37]; [31], [36] give an overview.

Whereas industrial MVac-LVdc SSTs have been found to be on par with LFT-based solutions regarding efficiency and volume [2], this paper evaluates the life-cycle environmental impacts, focusing on the embodied carbon footprint and the raw material usage, of MVac-LVdc interfaces realized either conventionally with an LFT and a LV ac-dc stage (**Fig. 1a**) or as an SST (**Fig. 1b**). The evaluation of the embodied carbon footprint and material usage is based on actually available/built systems/components as far as possible; specifically, a fully rated 13.2 kV, 400 kW first-generation industrial SST prototype [10] and a 1200 kVA second-generation SST demonstrator [38] are considered. First, **Section II** details the evaluated systems and the modeling approach, before **Section III** presents the comparative evaluation results. **Section IV** closes the paper with a discussion of the results and provides an outlook on further research.

II. MODELING

In general, LFT-based MVac-LVdc conversion, i.e., an LFT plus an LV ac-dc converter and hence referred to as “LFT+” in the following, and MVac-LVdc SSTs can achieve similar conversion efficiencies [2]. In the following, we consider LFT+ solutions with two different LFTs, i.e., a dry-type LFT compatible with Tier 2 efficiency requirements defined by the EU in [39] (Legrand GREEN T.HE series [40], [41]) as shown in **Fig 3a** and a high-efficiency dry-type transformer with an amorphous core, i.e., an amorphous metal distribution transformer (AMDT) [42] (ABB EcoDry Ultra series [43], [44]). The LV ac-dc conversion is modeled by scaling a 150 kW PV inverter (SMA Sunny High Power Peak 3) for which a detailed LCA study is available [19] to the rated power, e.g., of the considered 400 kW first-generation SST prototype [10] shown in **Fig 3b**.

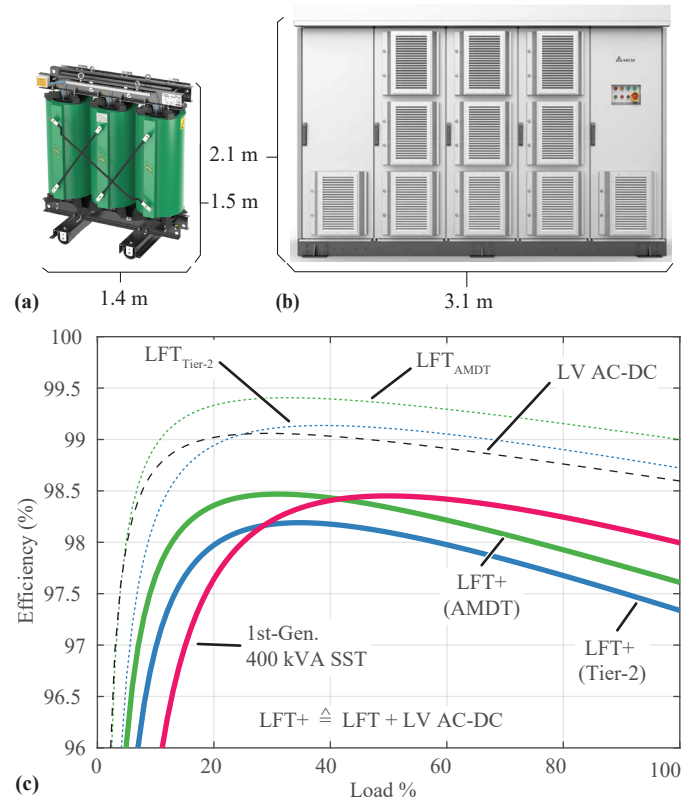


Fig. 3. Key elements of the considered 400 kW MVac-LVdc interfaces from **Fig. 1**. (a) 400 kVA dry-type LFT (image source: [40]) and (b) 400 kVA first-generation SST prototype [10] with the topology shown in **Fig. 1b**. (c) Efficiency curves of the considered MVac-LVdc interfaces from **Fig. 1** using directly measured values [10] of the 400 kW first-generation SST prototype shown in (b). The LFT-based solutions (referred to as “LFT+” in the following) are modeled by combining an LFT and a representative LV ac-dc converter [45], whereby two different dry-type LFT options are considered (Tier 2 efficiency according to EU regulations [39] or, alternatively, an ultra-efficient amorphous metal distribution transformer (AMDT) [43], [44]).

Fig. 3c shows the corresponding efficiency curves of the considered LFTs and the resulting LFT+ solutions and of the 400 kW first-generation SST prototype. Overall, both solutions can achieve similar efficiencies, especially if the LFT+ solution is realized using high-efficiency AMDTs. Note further that the efficiencies of LFTs increase with the rated power. Therefore, the carbon emissions during the use-phase due to the conversion losses, which are covered using the grid electricity mix with a non-zero carbon footprint per kWh, are similar and depend on the use case; therefore, the use phase is not considered further here but the focus is set on the embodied carbon footprint and the material usage.

In the following, the corresponding modeling approaches and assumptions are discussed on the example of the considered the 400 kW LFT+ and SST solutions, respectively. The embodied carbon footprints are either taken from available LCA studies and/or estimated based on the generic component models introduced in [32], which in turn are based on the literature and LCA databases like ecoinvent [46]; the ecoinvent database is also directly consulted for certain parts, materials, and processing steps.

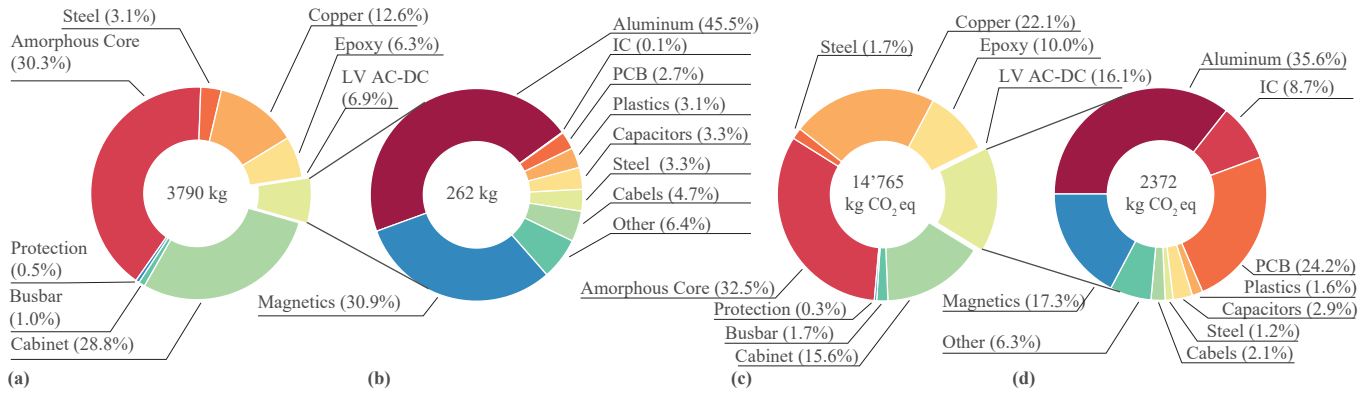


Fig. 4. (a) Weight and (b) embodied carbon footprint breakdown of the 400 kW LFT+ solution (see Fig. 1a) considering a high-efficiency AMDT LFT. The callouts give more details on the LV ac-dc converter using data from [19].

TABLE I
ESTIMATED MASS BREAKDOWNS OF DRY-TYPE TIER 2 AND AMDT LFTs (WITHOUT CABINET); THE ABSOLUTE VALUES ARE FOR 400 kVA UNITS.

Material	LFT Tier 2		LFT AMDT	
	Share	Mass	Share	Mass
Amorphous Core			65%	1550 kg
Steel	65.4%	1150 kg	5%	120 kg
Copper	< 0.1%	< 3 kg	20%	480 kg
Aluminum	22.3%	480 kg		
Epoxy	9.8%	130 kg	10%	240 kg
PET	2.5%	40 kg		
Total	100%	1350 kg	100%	2380 kg
η_{\max}	99.1%		99.4%	
$\eta_{400\text{kW}}$	98.7%		99.0%	

A. 400 kW LFT-based MVac-LVdc Interface (LFT+)

As mentioned, two realization options of a dry-type LFT are considered, i.e., an LFT with EU Tier 2 [39] efficiency levels and a high-efficiency AMDT with higher efficiency (see Fig. 3) which, however, is larger and heavier. Tab. I shows the corresponding material breakdowns, which are the basis for estimating the carbon footprint. For the considered Tier 2 dry-type LFT, detailed information on material composition is available from a product environmental profile (PEP) [41], whereas the mass breakdown of the AMDT is estimated based on [47], [48]. The overall weight of the AMDT is found via slight linear extrapolation of data of the ABB EcoDry Ultra series [43], [44]. As the amorphous core shows a lower saturation flux density compared to standard grain-oriented electrical steel (about 1.5 T instead of 2 T), the better efficiency of an AMDT comes at the price of higher material content and, for 400 kVA units, leads to an about 75% higher mass. The carbon footprint for the amorphous core material is assumed at 3.1 kg CO₂eq/kg [49] (i.e., about 30% higher than steel due to the required processing steps) and the ecoinvent database is consulted for all other material fractions.

The same MV-side input protection elements (except for the series inductor) used for the 400 kW first-generation SST prototype discussed below are considered. Similarly, an outdoor

cabinet housing the LFT and the protection elements is considered, and the corresponding amount of steel is obtained by scaling the data of the cabinet used for a 1200 kW second-generation SST (see Section III) via the required surface area (for the LFTs, the necessary cabinet size ensuring sufficient isolation distances etc. is available from the data sheets). Note that the more efficient but larger AMDT consequently requires a larger cabinet than the Tier 2 LFT.

The LV ac-dc converter is modeled based on an SMA Sunny High Power Peak 3 PV inverter [50] with a power rating of 150 kW, which includes a housing for outdoor mounting. The embodied carbon footprint is found by scaling the results of a detailed LCA study [19] to fit a 400 kW system. The LCA results were verified as far as possible using the material breakdowns provided therein and the generic component models introduced in [32], whereby an overall match within 10% has been found. Note that a PV inverter features additional power circuitry such as a maximum power point (MPP) tracker; i.e., a conservative estimate for the LV-side ac-dc converter of the LFT+ solution results.

Fig. 4a shows the resulting weight breakdown for a 400 kW LFT+ solution using a high-efficiency AMDT. The LFT and the cabinet (for the LFT and the input protection) contribute most of the total weight. For the ac-dc converter a more detailed weight breakdown is provided using the LCA data from [19]. In terms of weight, aluminum (heat sink etc.) and the magnetic components contribute around 75%. The weight of the copper bus bars in the LFT+ solution is assumed to be identical as in the SST where accurate numbers are provided.

The weight/material information is then translated into the embodied carbon footprint using the component models from [32] and available LCA data for the LV ac-dc converter. Fig. 4cd shows the resulting embodied carbon footprint breakdown. It is clearly visible that, e.g., the weight of printed circuit boards (PCBs) is almost negligible but contributes significantly to the carbon footprint. Similar observations can be made for integrated circuits (ICs; here including power semiconductors) due to the high energy intensity of the production. Consequently, the share of the LV ac-dc converter in the overall LFT+ carbon footprint is higher (16%) than its mass share (7%).

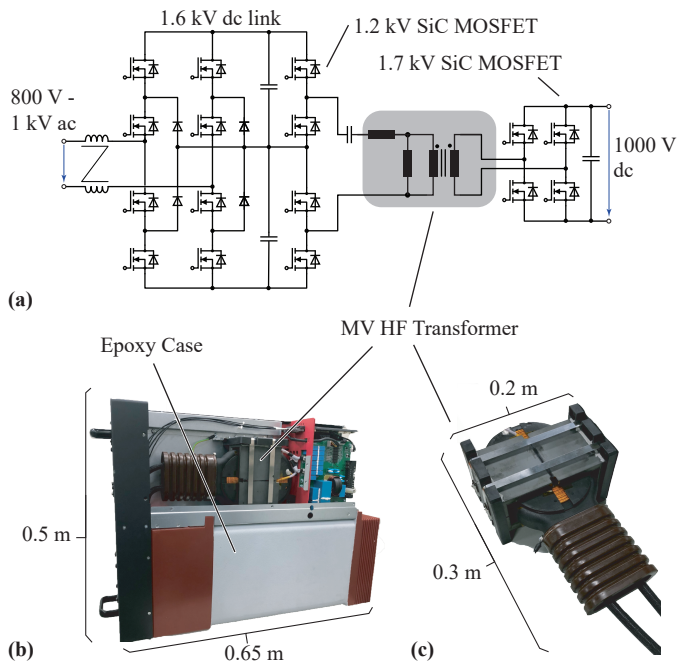


Fig. 5. (a) Power circuit of one 15 kW converter cell of the 400 kW first-generation SST demonstrator reported in [10] and shown in **Fig. 3b**, and photos of (b) the converter cell and (c) the HF transformer.

B. 400 kW First-Generation MVac-LVdc SST

The full-scale 400 kW first-generation SST prototype [10] shown in **Fig. 3b** features the power circuit topology from **Fig. 1b** and consists of 27 converter modules arranged in an input-series output-parallel (ISOP) configuration. As 9 modules share the MV grid phase voltage, each module only requires an ac input voltage of 800 V to 1 kV and a nominal power of 15 kW; the output dc voltage is 1 kV. The power circuit topology of a module is shown in **Fig. 5a** and consists of a 3-level neutral-point-clamped (NPC) single-phase ac-dc conversion stage followed by an isolated dc-dc converter. The dc-dc converter employs a 4-switch symmetric half-bridge (SHB) stage on the primary side of the HF transformer and a full-bridge on the secondary side. The module uses 1.2 kV SiC power transistors on the MV side and 1.7 kV SiC power transistors on the dc side. As the cells are connected in series on the MVac side and in parallel on the LVdc side, the HFT has to provide the galvanic isolation between MV and LV and thus must withstand the corresponding lightning impulse test voltages, hence the large bushings (see **Fig. 5c**). Similarly, the MV-side power electronics are encased in an epoxy box as shown in **Fig. 5b**. Finally, the overall SST features an MVac input section containing protection devices (fuses, surge arresters) and an input filter inductor. All 27 converter modules are interconnected by copper bus bars and, together with the the input protection, installed in a steel cabinet for outdoor use. Further implementation details are given in [10].

The material/weight breakdown of the SST prototype is found directly from the bill of materials (BOM). The carbon footprint of each converter cell is estimated using component

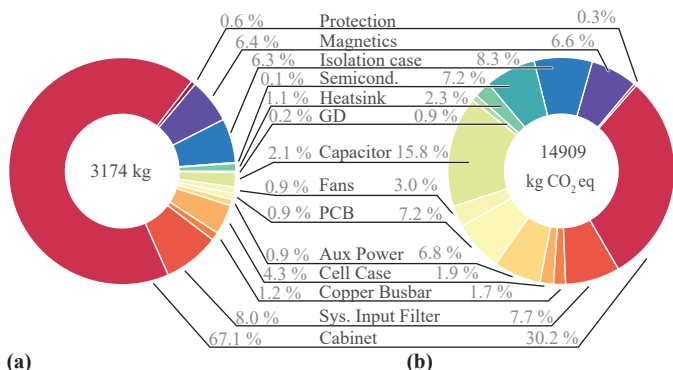


Fig. 6. (a) Mass and (b) embodied carbon footprint breakdowns of the 400 kW first-generation SST prototype reported in [10] and shown in **Fig. 3b**.

models described in [32], either via the electrical properties of the components (e.g., capacitance and voltage rating) or via measuring the mass of certain materials (e.g., copper winding of the HFT). The contributions of copper bus bars, protection devices, and the steel cabinet (for outdoor use) are considered via the respective materials and masses.

Fig. 6a presents the weight breakdown and **Fig. 6b** the breakdown of the embodied carbon footprint. It is evident that the cabinet / structural parts contribute significantly, accounting for approximately 67% of the total weight. Note that the magnetic components, i.e., the HFTs (see **Fig. 3c**) which are built using copper windings, ferrite cores, and epoxy isolation, only contribute about 6.4% of the total mass. Again, note that components such as power semiconductors have a minimal impact on the weight but substantially contribute to the overall carbon footprint, primarily due to the high energy intensity of their manufacturing process. Similar effects are observed for the PCBs, the auxiliary power units of the converter modules, and the capacitors.

III. COMPARATIVE EVALUATION

This section presents a comparative evaluation of the 400 kW LFT+ system and the first-generation SST discussed above, but also considers a 1200 kW second-generation SST demonstrator [38]. This optimized SST is shown in **Fig. 7** and consists of 30 modules in an ISOP arrangement. Each module has a nominal power rating of 40 kW and is depicted in **Fig. 7b**. Note that the overall volume is almost the same as that of the 400 kW first-generation SST prototype from **Fig. 3b**, i.e., the (volumetric) power density has been increased threefold, while similar efficiencies are achieved. Again, the mass and carbon footprint breakdowns of this SST are found based on the BOM and using the same procedure as discussed in **Section II-B**. Similarly, the results for a corresponding 1200 kW LFT+ solution are obtained as discussed above in **Section II-A**. In the following, all realization options are comparatively evaluated regarding mass, embodied carbon footprint, and raw material usage.

A. Mass

Fig. 8a presents the mass breakdowns of all considered MVac-LVdc interfaces, i.e., the LFT+ solution evaluated with

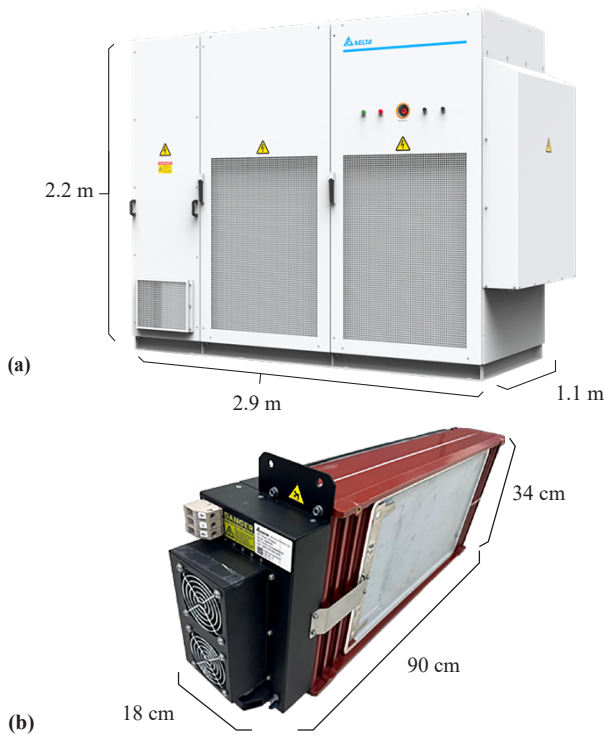


Fig. 7. (a) Photo of a 1200 kW second-generation SST demonstrator [38] and (b) detail view of one 40 kW converter cell. Note the SST's more than three times higher volumetric power density (6.9 MW/m^3) compared to the 400 kW first-generation SST prototype (2 MW/m^3) shown in Fig. 3b.

both, an ultra-efficient AMDT LFT and a standard Tier 2 LFT, for rated power levels of 400 kW and 1200 kW, as well as the 400 kW first-generation and the 1200 kW second-generation SSTs. As previously discussed, the weight of the LFT+ systems is dominated by the LFT and the cabinet. When comparing the 400 kW and 1200 kW LFT+ realizations, note that the absolute masses of the cabinets and the LFTs do not increase in proportion to the rated power because the size of an LFT and in particular its surface area do not scale linearly with power. Interestingly, the overall weight of the 1200 kW second-generation SST is lower than that of the 400 kW first-generation SST despite the three times higher power rating; clearly, the 400 kW first-generation SST was a prototype designed primarily to demonstrate the viability of the concept for applications such as EV charging, but without significant optimization. For example, the cabinet contributes around two-thirds of the total weight of the 400 kW SST whereas the cabinet contribution is significantly reduced in the optimized 1200 kW second-generation SST.

Fig. 8b displays the mass breakdowns in terms of specific weight, i.e., in kilograms per kilowatt of rated power, which confirms the expectation that systems with higher nominal power feature an improved specific weight (less kg/kW). This is intuitive, as certain components such as cabinets, protective elements, and mechanical support structures do not scale with power, and in case of the LFT+ solutions also because of the favorable scaling of LFT volume/weight with power rating

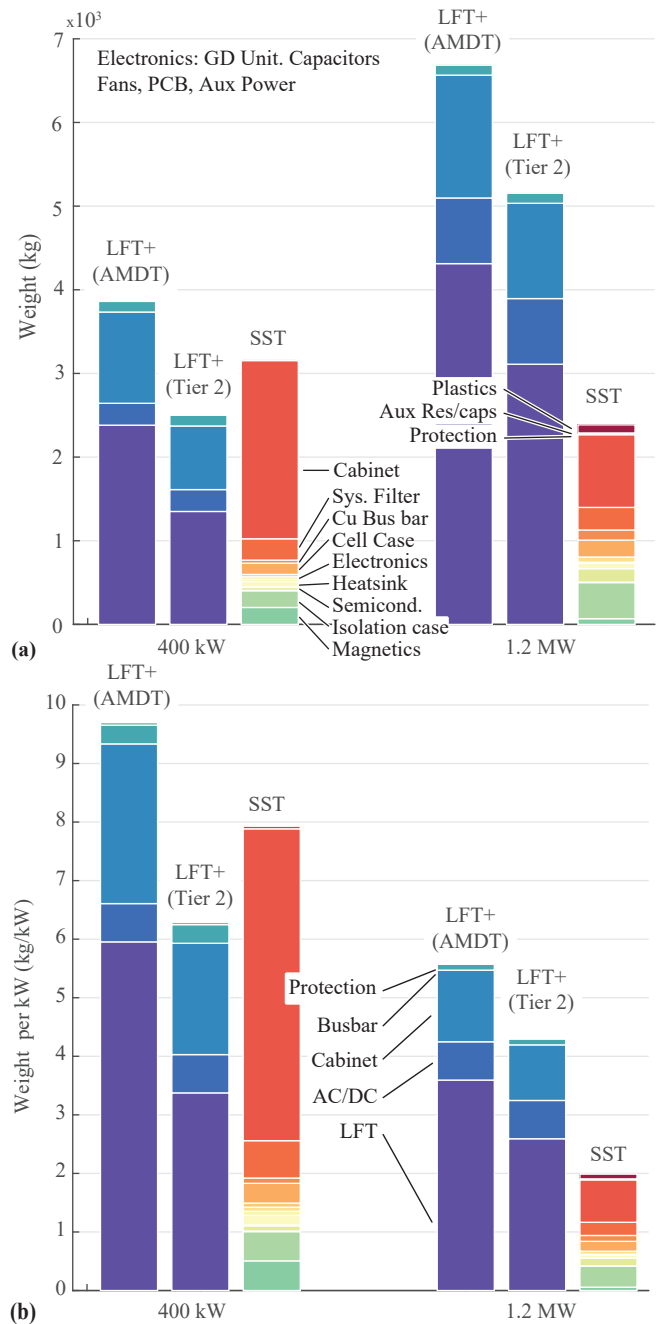


Fig. 8. Weight comparison of the considered MVac-LVdc conversion systems in (a) absolute terms and (b) normalized to the rated power (specific weight). Two different realization options are considered for the dry-type LFT, whereby the AMDT variant is more efficient but heavier compared to an LFT with Tier-2 efficiency levels according to EU regulations [39]. Further, the specific weight of the LFTs improve with the rated power. Note the significant improvement in material efficiency of the 1200 kW second-generation SST demonstrator from Fig. 7 compared to the 400 kW first-generation SST prototype from Fig. 3b. Further, note that in the 1200 kVA class, the SST weight is only about 1/3 of that of the LFT+ solutions.

mentioned above. For a given power rating, the two LFT+ solutions differ in terms of specific weight depending on whether a Tier 2 LFT or a heavier (but more efficient, see Fig. 3) AMDT LFT is used. Finally, the 1200 kW second-generation

SST demonstrator only shows about 1/3 of the weight of the LFT+ solutions.

B. Embodied Carbon Footprint

Fig. 9a shows the embodied carbon footprints of all six MVac-LVdc interfaces. As discussed previously, the contributions of the components/subsystems to the carbon footprints is quite different than the respective weight contributions; e.g., because 1 kg of steel has a much lower carbon footprint than 1 kg of PCB. The LFTs account for about 2/3 of the LFT+ solutions' carbon footprints due to the high raw material content / large mass. In contrast, the contribution of the SSTs' HFTs to the embodied carbon footprint is comparably low but the large amount of electronic components (power semiconductors, capacitors for the buffering of the single-phase power flow in the phase-modular SST topology from **Fig. 1b**, PCBs, etc.) dominate.

Fig. 9b then shows the specific carbon footprints, i.e., the embodied carbon footprint normalized to the rated power. Similar trends as for the mass can be observed: Systems with higher rated power generally require less material (better material efficiency / lower mass), which translates into a lower carbon footprint. Still, the LFT (and its cabinet) contributes a significant part of the LFT+ solutions' carbon footprints, and there is little room for further improvement of that share; thus even if the LV ac-dc converter's specific carbon footprint could be reduced in the future, the LFT imposes a lower bound. In contrast, the clear improvement of the 1200 kW second-generation SST demonstrator compared to the 400 kW first-generation SST prototype confirms the potential of SST technology to benefit from improvements in power electronics, whereas the LFT+ solutions ultimately are remain constrained by the material usage.

C. Resource Usage

Efficient use of materials is crucial for reducing environmental impact and conserving finite resources. Prioritizing resource efficiency also lowers costs, supports sustainability, and ensures compliance with environmental regulations. **Fig. 10a** illustrates the copper usage in all three 1200 kW MVac-LVdc interfaces. The high-efficiency AMDT LFT uses copper windings; otherwise, mainly the busbars contribute to the copper usage. **Fig. 10b** shows the aluminum usage. Note that the Tier 2 LFT employs aluminum windings. Both, the LFT+ solution's LV ac-dc converter and the SST employ heat sinks. **Fig. 10c** shows that the steel usage of the LFT+ solutions is much higher than that of the SST because of the LFTs' magnetic cores.¹ Further, in all three systems, the cabinet remains a dominant contributor to the steel usage. Finally, **Fig. 10d** presents the usage of epoxy, which serves primarily as an insulation material, e.g., in the LFTs and the SST's HFTs and isolation covers of the cells. Interestingly, all three systems require similar total amounts of epoxy.

¹Note that the amorphous metal core of the AMDT is considered as steel here even though further processing steps are needed compared to conventional grain-oriented electrical steel.

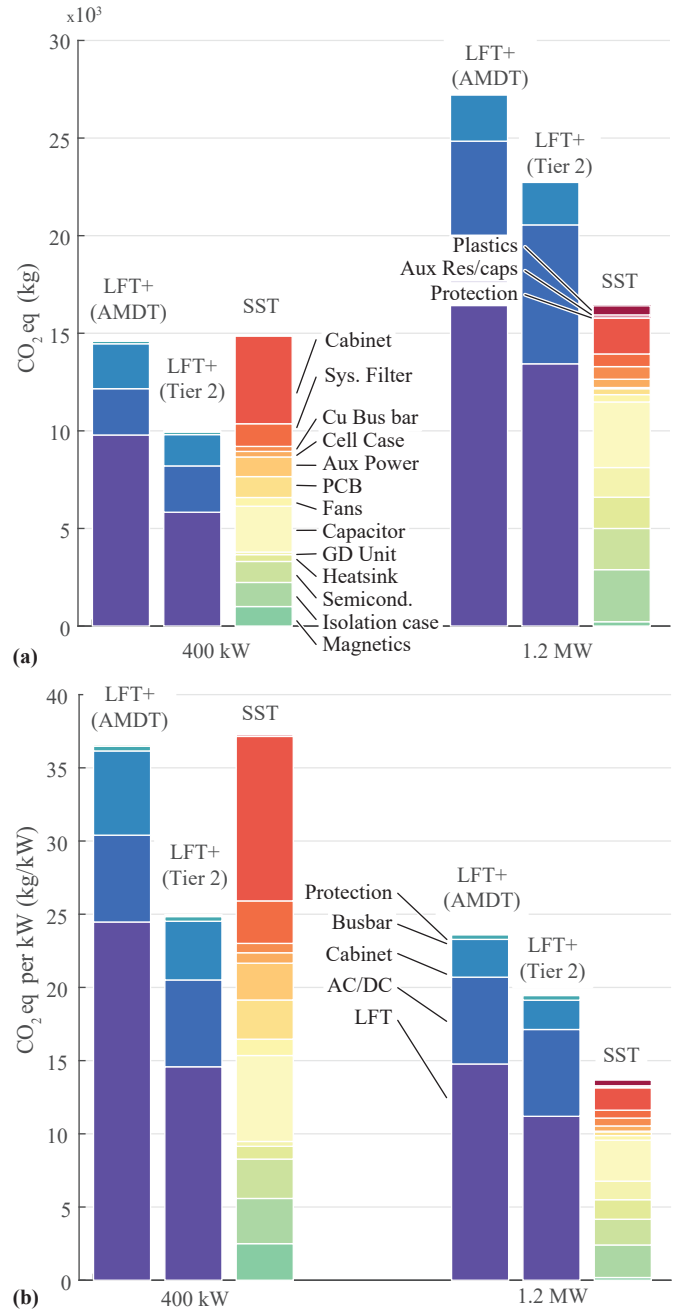


Fig. 9. Comparison of the embodied carbon footprints of the considered MVac-LVdc conversion systems in (a) absolute terms and (b) normalized to the rated power (specific carbon footprint). Two different realization options are considered for the dry-type LFT, whereby the AMDT LFT is more efficient but heavier compared to an LFT with Tier-2 efficiency levels according to EU regulations [39]; the higher weight translates to a higher embodied carbon footprint. Note the significant improvement in the specific embodied carbon footprint of the 1200 kW second-generation SST demonstrator from **Fig. 7** compared to the first-generation 400 kW first-generation SST prototype from **Fig. 3b**. Further, note that in the 1200 kVA class the embodied carbon footprint of the SST is only about half that of the LFT+ solution with the high-efficiency AMDT transformer, which is expected to show comparable efficiencies in operation (see **Fig. 3**).

IV. DISCUSSION AND CONCLUSION

MVac-LVdc SSTs, e.g., for high-power EV charging, achieve similar efficiencies and power densities as LFT-based solutions.

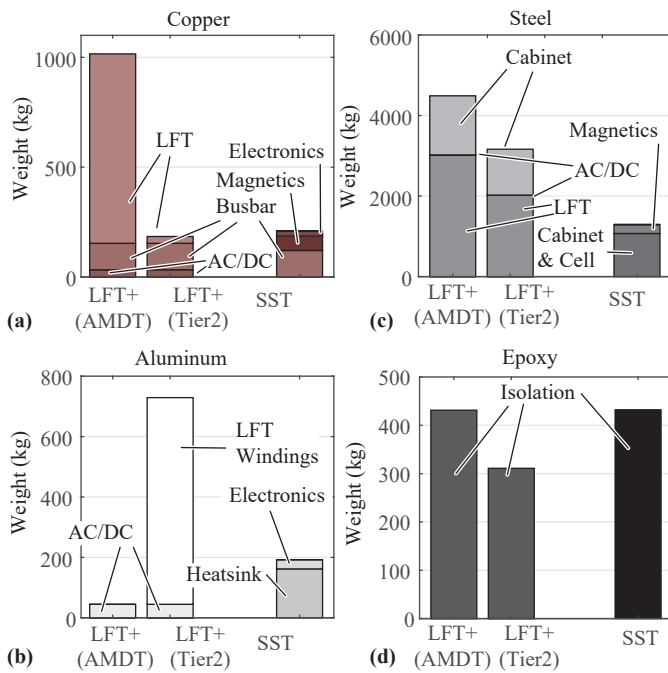


Fig. 10. Material usage of 1200kW LFT+ MVac-LVdc interfaces and the 1200kW second-generation SST demonstrator from Fig. 7. (a) Copper; (b) steel; (c) aluminum; (d) epoxy. Note that the Tier 2 LFT uses aluminum windings and the AMDT LFT employs copper windings.

This paper, for the first time, provides a comparative evaluation of the embodied carbon footprints and material usage, based on the BOMs of actually built industrial SST demonstrator systems.

LFTs have been optimized during decades of research and development, leaving little room for further improvements. Hence, there are lower bounds for the material usage and the embodied carbon footprint of LFT-based solutions. In contrast, SSTs are still in an evolving phase, which provides ample opportunities to enhance performance while minimizing material consumption and embodied carbon footprint, e.g. advances in semiconductor technology, high-frequency magnetics, and cooling systems offer pathways to reduce the mass and energy intensity of future SST designs. Additionally, the modular nature of SSTs allows for greater flexibility and leverages economies of scale. This is reflected by the massive reduction of the specific carbon footprint of the considered 1200 kW second-generation SST demonstrator (13.7 kg CO₂eq/kW, i.e., about 2/3 of an equivalent LFT-based solution) compared to its first-generation counterpart (37.3 kg CO₂eq/kW).

Whereas SSTs thus have the potential to outperform LFT-based solutions of similar efficiency in terms of material usage and embodied carbon footprint, LFTs typically achieve very long service lives of 40 years and beyond, i.e., more than the power electronics (typ. 20 years). However, for the considered 1200 kW systems, even if the SST and the LV ac-dc converter of the LFT-based solution must be replaced once to reach a lifetime of 40 years, the overall embodied carbon footprint of the LFT-based solution (29.6 kg CO₂eq/kW) is still slightly

higher than that of the two SSTs (27.3 kg CO₂eq/kW). Further, the modular structure of the SST simplifies maintenance and repair, i.e., only faulty modules could be replaced instead of the entire system.

On the other hand, LFTs may show a high material usage, but their relatively simple construction facilitates very high end-of-life recycling rates of 80...90% [41]. Thus, aspects such as reliability, reuse of components, recyclability and, in general, the compatibility with future circular economy concepts should be targeted by further research. Furthermore, also hybrid solutions with partial power processing (e.g., an LFT with a 12-pulse thyristor rectifier and a small LV ac-dc converter acting as an active filter [2], [51]) should be included in the comparison.

ACKNOWLEDGMENT

The Advanced Mechatronic Systems Group at ETH Zürich is generously supported by the *Else und Friedrich Hugel Fonds* via the *ETH Zurich Foundation*, for which the authors are most grateful. The authors would also like to thank the *European Center for Power Electronics e.V. (ECPE)* for the financial support. Further, the authors would like to thank Eddie Huang and Johnny Yeh from the Delta Taiwan team for providing the details of the data used in this paper.

REFERENCES

- [1] C. Zhao, D. Dujic, A. Mester, J. K. Steinke, M. Weiss, S. Lewden-Schmid, T. Chaudhuri, and P. Stefanutti, "Power electronic traction transformer—Medium voltage prototype," *IEEE Trans. Ind. Electron.*, vol. 61, no. 7, pp. 3257–3268, Jul. 2014.
- [2] J. Huber, P. Wallmeier, R. Pieper, F. Schafmeister, and J. W. Kolar, "Comparative evaluation of MVAC-LVDC SST and hybrid transformer concepts for future datacenters," in *Proc. Int. Power Electron. Conf. (IPEC/ECCE Asia)*, Himeji, Japan, May 2022, pp. 2027–2034.
- [3] R. Unruh, F. Schafmeister, N. Froehleke, and J. Boecker, "1-MW full-bridge MMC for high-current low-voltage (100V-400V) DC-applications," in *Proc. Power Convers. Intelligent Motion Conf. (PCIM)*, Nuremberg, Germany, Jul. 2020.
- [4] "Milestones of Sungrow: 2022," 2022. [Online]. Available: <https://en.sungrowpower.com/AboutSungrow/1/introduction>
- [5] S. Srdic and S. Lukic, "Toward extreme fast charging: Challenges and opportunities in directly connecting to medium-voltage line," *IEEE Electr. Mag.*, vol. 7, no. 1, pp. 22–31, Mar. 2019.
- [6] H. Tu, H. Feng, S. Srdic, and S. Lukic, "Extreme fast charging of electric vehicles: A technology overview," *IEEE Trans. Transp. Electr.*, vol. 5, no. 4, pp. 861–878, Dec. 2019.
- [7] A. Meintz, M. Starke, and T. Bohn, "Charging infrastructure technologies: Development of a multiport, >1 MW charging system for medium- and heavy-duty electric vehicles," presented at the DOE Vehicle Techn. Program Annu. Merit Rev. Peer Eval. Meet., Jan. 2021. [Online]. Available: <https://www.nrel.gov/docs/fy22osti/79988.pdf>
- [8] K. Pouresmaeil, J. Duarte, K. Wijnands, M. Roes, and N. Baars, "Single-phase bidirectional VZCS AC-DC converter for MV-connected ultra-fast chargers," in *Proc. Power Convers. Intelligent Motion Conf. (PCIM)*, Nuremberg, Germany, May 2022.
- [9] K. Nakatsu, T. Kumazaki, A. Kanouda, K. Ide, and T. Tsukishima, "Development of smart power management for achieving carbon neutrality by 2050: Energy ecosystems for widespread EV adoption," *Hitachi Rev.*, vol. 71, no. 1, pp. 51–57, 2022.
- [10] C. Zhu, "High-efficiency, medium-voltage-input, solid-state-transformer-based 400-kW/1000V/400A extreme fast charger for electric vehicles," Tech. Rep. EE-0008361, Jul. 2023. [Online]. Available: <https://www.osti.gov/servlets/purl/1987553/>

- [11] J. Yu, C. Luo, J. Duan, C. Wang, R. Lu, A. Trujillo, C. Li, and W. Li, "Design and validation of a 2MW 10kV medium-voltage solid state transformer," in *Proc. Energy Convers. Congr. Expo (ECCE USA)*, Phoenix, AZ, USA, Oct. 2024.
- [12] Statista, "Copper annual market price 2022." [Online]. Available: <https://www.statista.com/statistics/533292/average-price-of-copper/>
- [13] U.S. Geological Survey (USGS), "Metal prices in the United States through 2010," Scientific Investigations Report 2012–5188, 2013. [Online]. Available: <https://pubs.usgs.gov/sir/2012/5188/>
- [14] Fraunhofer ISE, "Current and future cost of photovoltaics. long-term scenarios for market development, system prices and LCOE of utility-scale PV systems," Study on behalf of Agora Energiewende, Feb. 2015. [Online]. Available: <https://www.agora-energiewende.org/publications/current-and-future-cost-of-photovoltaics>
- [15] European Commission, "The European green deal." [Online]. Available: https://commission.europa.eu/strategy-and-policy/priorities-2019-2024/european-green-deal_en
- [16] —, "Circular economy action plan." [Online]. Available: https://environment.ec.europa.eu/strategy/circular-economy-action-plan_en
- [17] F. Musil, C. Harringer, A. Hiesmayr, and D. Schönmayr, "How life cycle analyses are influencing power electronics converter design," in *Proc. Power Convers. Intelligent Motion Conf. (PCIM Europe)*, Nuremberg, Germany, May 2023.
- [18] Fronius International GmbH, "Fronius Tauro – Nachhaltige Technologie für eine grüne Zukunft: Lebenszyklusanalyse, (in German)," 2022. [Online]. Available: [https://www.fronius.com/~downloads/Solar%20Energy/Whitepaper/SE_WP_LCA_Tauro_DE.pdf](https://www.fronius.com/~/downloads/Solar%20Energy/Whitepaper/SE_WP_LCA_Tauro_DE.pdf)
- [19] SMA Solar Technology AG, "Sunny Highpower PEAK3 life cycle assessment (LCA)," Jun. 2023. [Online]. Available: <https://files.sma.de/assets/280662.pdf>
- [20] —, "Sunny Central 4600 UP life cycle assessment (LCA)," Oct. 2024. [Online]. Available: <https://www.sma.de/en/newsroom/news-details/life-cycle-assessment-sunny-central-up-sustainability-performance>
- [21] J. Popović-Gerber, J. A. Ferreira, and J. D. van Wyk, "Quantifying the value of power electronics in sustainable electrical energy systems," *IEEE Trans. Power Electron.*, vol. 26, no. 12, pp. 3534–3544, Dec. 2011.
- [22] A. Nordelöf, M. Alatalo, and M. L. Söderman, "A scalable life cycle inventory of an automotive power electronic inverter unit—Part I: Design and composition," *Int. J. Life Cycle Assess.*, vol. 24, no. 1, pp. 78–92, Jan. 2019. [Online]. Available: <https://doi.org/10.1007/s11367-018-1503-3>
- [23] G. A. Quintana-Pedraza, S. C. Vieira-Agudelo, and N. Muñoz-Galeano, "A cradle-to-grave multi-pronged methodology to obtain the carbon footprint of electro-intensive power electronic products," *Energies*, vol. 12, no. 17, p. 3347, Jan. 2019.
- [24] C. Hunziker, J. Lehmann, T. Keller, T. Heim, and N. Schulz, "Sustainability assessment of novel transformer technologies in distribution grid applications," *Sustain. Energy Grids Netw.*, vol. 21, p. 100314, Mar. 2020.
- [25] M. Patra, T. Cormenier, A. Louise, and P. Murlon, "European ecodesign material efficiency standardization supporting circular economy aspects of power drive systems for sustainability," in *Proc. 12th Int. Conf. Energy Efficiency Motor Driven Syst. (EEMODS)*, Stuttgart, Germany, May 2022.
- [26] T. T. Romano, T. Alix, Y. Lembeye, N. Perry, and J.-C. Crebier, "Towards circular power electronics in the perspective of modularity," *Procedia CIRP*, vol. 116, pp. 588–593, Jan. 2023.
- [27] B. Baudais, H. Ben Ahmed, G. Jodin, N. Degrenne, and S. Lefebvre, "Life cycle assessment of a 150 kW electronic power inverter," *Energies*, vol. 16, no. 5, p. 2192, Jan. 2023.
- [28] S. Glaser, P. Feuchter, and A. Diaz, "Looking beyond energy efficiency - Environmental aspects and impacts of WBG devices and applications over their life cycle," in *Proc. Europ. Power Electron. Conf. (EPE)*, Aalborg, Denmark, Sep. 2023.
- [29] L. B. Spejo, I. Akor, M. Rahimo, and R. A. Minamisawa, "Life-cycle energy demand comparison of medium voltage silicon IGBT and silicon carbide MOSFET power semiconductor modules in railway traction applications," *Power Electron. Dev. Comp.*, vol. 6, p. 100050, Oct. 2023.
- [30] L. Vauche, G. Guillemaud, J.-C. Lopes Barbosa, and L. Di Cioccio, "Cradle-to-gate life cycle assessment (LCA) of GaN power semiconductor device," *Sustainability*, vol. 16, no. 2, p. 901, Jan. 2024.
- [31] J. Huber, L. Imperiali, D. Menzi, F. Musil, and J. W. Kolar, "Energy efficiency is not enough!" *IEEE Power Electron. Mag.*, vol. 11, no. 1, pp. 18–31, Mar. 2024.
- [32] L. Imperiali, D. Menzi, J. W. Kolar, and J. Huber, "Multi-objective minimization of life-cycle environmental impacts of three-phase AC-DC converter building blocks," in *Proc. IEEE Appl. Power Electron. Conf. Expo. (APEC)*, Long Beach, CA, USA, Feb. 2024.
- [33] C. Minke, R. Mallwitz, P. Burfeind, and D. Hu, "Recycling potential of power electronics solutions - An exemplary study about on-board chargers," in *Proc. 13th Int. Conf. Integrated Power Systems (CIPS)*, Düsseldorf, Germany, Mar. 2024.
- [34] K. Ribeiro de Faria, J.-R. Capounda, V. Rajagopal, P. Menegazzi, B. Paul, N. Kamil, S. Galeshi, and N. Messi, "Efficiency, volume and CO₂ emissions impact in a PFC converter with an active filter solution for OBC application," in *Proc. Power Convers. Intelligent Motion Conf. (PCIM Europe)*, Nuremberg, Germany, Jun. 2024.
- [35] L. Fang, E. Quisbert-Trujillo, P. Lefranc, and M. Rio, "Leading LCA result interpretation towards efficient ecodesign strategies for power electronics: The case of DC-DC buck converters," *Procedia CIRP*, vol. 122, pp. 731–736, Jan. 2024.
- [36] F. Salomez, H. Helbling, M. Almanza, U. Soupremanien, G. Viné, A. Voldoire, B. Allard, H. Ben-Ahmed, D. Chatroux, A. Cizeron, M. Delhommiais, M. Fayolle-Lecocq, V. Grennerat, P.-O. Jeannin, L. Laudebat, B. Rahmani, P.-E. Vidal, L. Villa, L. Dupont, and J.-C. Crébier, "State of the art of research towards sustainable power electronics," *Sustainability*, vol. 16, no. 5, p. 2221, Jan. 2024.
- [37] A. Campos, A. Jasi, K. Verzhinin, and P. Dworakowski, "CO₂ footprint of medium voltage DC solid state transformer," in *Proc. Power Convers. Intelligent Motion Conf. (PCIM Europe)*, Nuremberg, Germany, Jun. 2024.
- [38] Delta Electronics, Inc., "Solid-state transformers (SST): Enabling smarter and more efficient grid," 2024. [Online]. Available: <https://www.deltaww.com/en-US/products/solid-state-transformer/ALL/>
- [39] The European Commission, "Commission regulation (EU) 548/2014," May 2014. [Online]. Available: <https://eur-lex.europa.eu/eli/reg/2014/548/oj>
- [40] Legrand SA, "Green T.HE cast resin transformers," 2021. [Online]. Available: https://datacenter.legrandwebfactory.com/sites/g/files/ocwmcrr716/files/2023-06/Green_T.HE_Transformer_Brochure_16770.pdf
- [41] —, "Product environmental profile: Green transformers high efficiency TIER2," Apr. 2021. [Online]. Available: https://www.legrand.co.uk/sites/g/files/ocwmcrr866/files/2023-07/btcino_green_he_transformer_tier2_lgrp-01351-v01.01-en.pdf
- [42] M. Carlen, D. Xu, J. Clausen, T. Nunn, V. R. Ramanan, and D. M. Getson, "Ultra high efficiency distribution transformers," in *Proc. IEEE PES Transm. Distr. Conf. Expo. (PES T&D)*, New Orleans, LA, USA, Apr. 2010.
- [43] ABB, "Technical data EcoDry dry-type transformers," 2013.
- [44] ABB Ltd., "EcoDry: Ultra-efficient dry-type transformers—Lower environmental impact while cutting your costs," 2011. [Online]. Available: <https://library.e.abb.com/public/e6deb4eb2025aa348257c000016fc6f11de000076%20en%20ecodry%20dry-type%20transformers%20final.pdf>
- [45] SMA Solar Technology AG, "Sunny Boy US / Sunny Tripower US / Sunny Highpower US: Efficiency and derating," Oct. 2018. [Online]. Available: <https://files.sma.de/downloads/WKG-Derating-US-TI-en-20.pdf>
- [46]ecoinvent, "Ecoinvent Database 3.9.1." [Online]. Available: <https://ecoinvent.org/>
- [47] M. Carlen, U. Överström, V. V. Ramanan, J. Tepper, L. Swanström, P. Klys, and E. Stryken, "Life cycle assessment of dry-type and oil-immersed distribution transformers with amorphous metal core," in *Proc. 21st Int. Conf. Electricity Distrib.*, Frankfurt, Germany, Jun. 2011.
- [48] L. de Oliveira, M. Özerten, G. Kablouti, and A. Nogués, "The sustainability benefits of liquid cooled dry-type transformers in renewable energy and vent-closed applications," in *Proc. CIGRE Session*, Paris, France, Aug. 2024.
- [49] Proterial, Ltd., "Issuance of a life cycle assessment (LCA) report for amorphous alloy MaDC-a™," Oct. 2024. [Online]. Available: <https://www.proterial.com/e/press/2024/n1030b.html>
- [50] SMA Solar Technology AG, "Sunny Highpower Peak3 - Customized for tomorrow today," Datasheet. [Online]. Available: <https://files.sma.de/downloads/SHP-20-DS-en-22.pdf>
- [51] M. Schulz, D. Hoffmann, and M. Ketterer, "The resurrection of GTOs and thyristors as core components in MW-charger-application and railway/mining refurbishment," in *Proc. Power Conversion and Intelligent Motion Conf. (PCIM Europe)*, Nuremberg, Germany, May 2022.